Basic insights into ALD conformality

A closer look at ALD and thin film conformality

Please cite as: K. Arts, W.M.M. Kessels and H.C.M Knoops. Basic insights into ALD conformality – A closer look at ALD and thin film conformality. **2020**, 1. AtomicLimits

Animations can be downloaded at AtomicLimits.com

Investigating the conformality of thin films grown by atomic layer deposition (ALD) is not only interesting from an applications perspective. It can also provide valuable fundamental information, for example about reaction probabilities.[1,2] Personally, I became aware of this during my (still ongoing) PhD work in the Plasma and Materials Processing group at the Eindhoven University of Technology. Within our NWO-TTW project entitled 'Taking Plasma ALD to the Next Level' we try to tackle several fundamental aspects of (plasma) ALD, and studying film conformality turned out to be a powerful way of doing so.

Now, why this blog post? Primarily, we noticed that already known concepts, such as reaction-, diffusion- and recombination-limited growth,[3] can still be difficult to explain. Therefore we made instructive figures and animations and then I thought it would be good to share these online. Moreover, the insights that are summarized can also be used as guidelines for optimizing film conformality during (plasma) ALD. Further details on how we used these insights in experiments can be found in our recent papers.[1,2]

One of the most important messages here is that the loss of reactant molecules through surface adsorption and surface recombination may seem similar, but results in very different growth behavior. This is explained in the three following sections. First, the general approach for modeling ALD conformality, in terms of sticking probabilities and recombination probabilities, is described. Then, we show how the sticking probability determines the growth regime during thermally-driven ALD. Finally, we demonstrate how the recombination probability can limit film conformality during plasma ALD, where we note that plasma ALD can yield very conformal films as well.

Modeling ALD conformality: diffusion, adsorption and recombination

To relate film conformality during ALD to fundamental parameters such as reaction probabilities, you need a numerical or analytical model that describes the growth process in terms of these parameters. As recently reviewed by Cremers *et al.*,[4] several of such models have been reported in the literature. Many of these have been inspired by the analytical model introduced by Gordon in 2003,[5] which could adequately predict the minimal reactant dose needed to conformally coat a high-aspect-ratio (high-AR) hole, in the case of diffusion-limited growth (explained in the next section). Without going into the details and different approaches of the reported models, it is worth mentioning that essentially all of these simulate the *surface coverage θ* obtained during one ALD half-cycle. Experimentally, this surface coverage, or the 'reacted fraction of available adsorption sites', can be related to the growth per cycle (GPC) and therefore the thickness of the deposited film, as illustrated in figure 1.
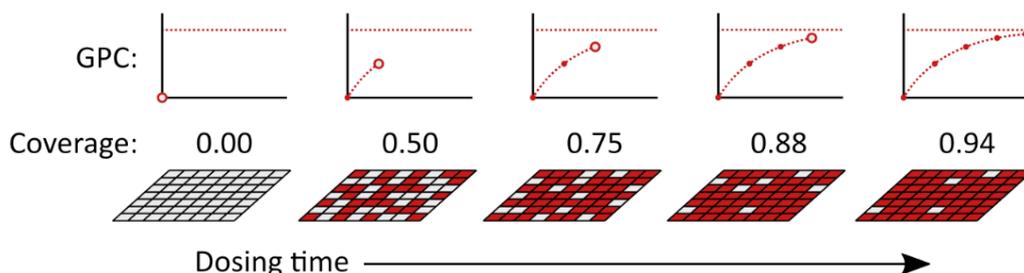

Figure 1: Surface coverage θ and GPC as a function of dosing time during one ALD half-cycle.

Here, I would like to focus on results obtained using the model that I have used in my research, which is based on the work of Yanguas-Gil and Elam.[6] This continuum model consists of two coupled equations: 1) the famous Langmuir equation describing irreversible adsorption, and 2) a one-dimensional diffusion equation to calculate the gas-phase reactant density inside the high-AR structure.

The irreversible adsorption of gas-phase reactant molecules is described using a *sticking probability s*: the probability that the reactant molecule irreversibly adsorbs or 'sticks' to the surface upon collision. Note that this probability should be zero in saturation, so when the surface coverage θ is equal to 1. If not, growth continues and we're modeling chemical vapor deposition (CVD) rather than ALD. In the adopted Langmuir model, the self-terminating behavior of ALD is modeled using $s = s_0(1 - \theta)$. Here, s_0 is the *initial sticking probability*: the sticking probability corresponding to the starting surface before dosing the reactant of the modeled half-cycle. Depending on the ALD process, the initial sticking probability generally lies in the range of 10^{-5} up to 10^{-1}.[1,3,4] This means that the reactant molecules can collide with the surface about 10 to 100 000 times (!) before irreversible adsorption takes place.

Next to adsorption, gas-phase reactant species can also be lost to the surface through recombination. This can occur in plasma ALD, where the reactive plasma radicals can recombine to form stable molecules that do not contribute to film growth. For example, atomic oxygen (O) can recombine to form stable, molecular O_2. Similarly, during ozone-based ALD the reactive ozone can also be lost through surface reactions forming molecular O_2.[7] In either case, this loss channel is modeled using a *surface recombination probability r*: the probability that the reactant molecule (or atom) recombines upon collision with the surface. Similar to the initial sticking probability of a precursor or co-reactant, the surface recombination probability of plasma radicals usually lies in the range of 10^{-5} up to 10^{-1}.[2–4]

There are two major differences between 'adsorption loss' and 'recombination loss', schematically illustrated in figure 2 (II$_a$ and II$_b$). First of all, adsorption reactions result in film growth, so an increase in surface coverage, while recombination reactions do not. Secondly, the adsorption loss stops when saturation is approached, such that the reactant molecules can diffuse deeper into the high-AR structure until they find available, unreacted adsorption sites. In contrast, recombination loss continues everywhere in the structure and therefore tends to be dominant.
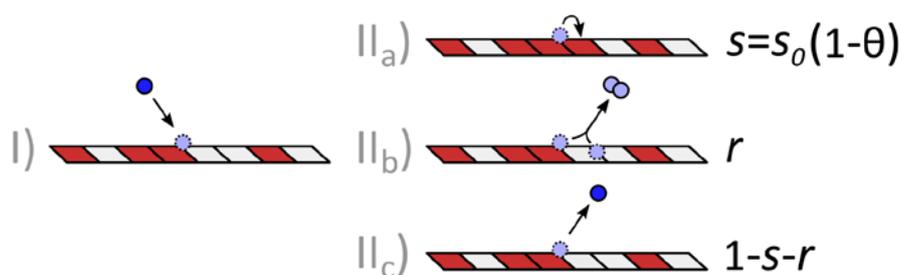

Figure 2: Illustration of the modeled interaction between gas-phase reactant species (blue circles) and the surface during (plasma) ALD, where the squares represent empty (white) and occupied (red) adsorption sites. When a reactant molecule or atom hits the surface (I), it can adsorb at an empty adsorption site (II$_a$), recombine with another atom at the surface (II$_b$) or reflect (II$_c$). Only adsorption (II$_a$) leads to an increase in surface coverage.

The initial sticking probability s_0 and the recombination probability r are important parameters determining the growth regime and resulting film conformality. These different growth regimes are discussed below, where simulation results are shown assuming 'single particle', free molecular diffusion in a narrow trench (i.e., with gap height $h \ll$ trench width, see figure 3). Although real-life cases are usually more complicated, think of gas-phase collisions, complex 3D geometries etc., the overall behavior is generic in nature and often realistic, particularly at low pressures (e.g., <1 Torr for µm-scale pores or trenches).[1,2]

Thermal ALD: reaction-limited versus diffusion-limited growth

In the case of thermally-driven ALD, recombination typically does not play a role ($r = 0$) and we can distinguish two different growth regimes: reaction-limited growth and diffusion-limited growth.[3,6,8] The difference between reaction- and diffusion-limited growth is illustrated in figure 3. In reaction-limited growth (left), the adsorption of gas-phase reaction molecules takes more time than the diffusion of these molecules into the high-AR structure. In diffusion-limited growth (right), the reactant molecules already adsorb before they have diffused all the way to the end of the structure. As you might guess based on this description, the ratio between the *diffusion time* t_{diff} and the *adsorption time* t_{ads} determines whether the film growth is reaction-limited ($\frac{t_{diff}}{t_{ads}} \ll 1$) or diffusion-limited ($\frac{t_{diff}}{t_{ads}} \gg 1$).
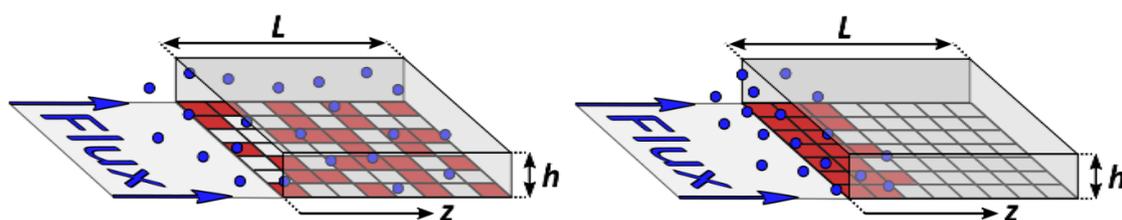

Figure 3: Illustration of reaction-limited growth (left) and diffusion-limited growth (right).

Here, we use *diffusion time* as the time needed for a reactant molecule to diffuse to the end of the high-AR structure. For 'random walk' diffusion during a time t, the average penetration depth of the reactant molecules increases with $\sqrt{t}$. Correspondingly, the time it takes to reach the end of the structure increases with the aspect ratio squared, so $t_{diff} \propto \text{AR}^2$ where $\text{AR} = L/h$.
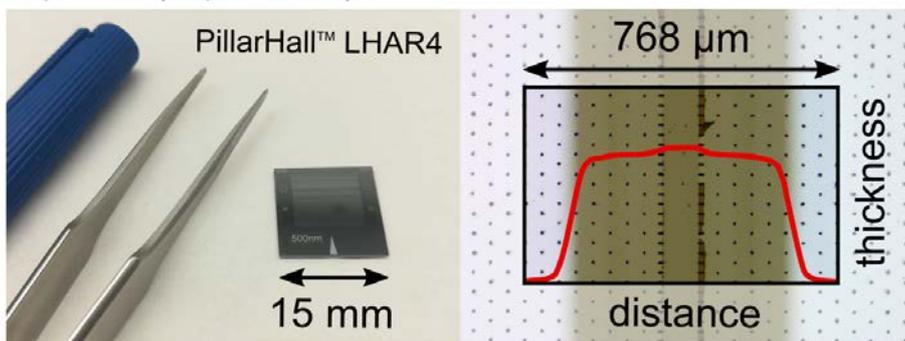
With *adsorption time* we refer to the time it takes to 'fill up' a certain fraction of adsorption sites. Regardless of what fraction this is (1/e, 0.5, 0.9999...), the adsorption time is proportional to the average number of collisions needed for an adsorption reaction to occur. On the initial, empty surface, this number of collisions is equal to $1/s_0$. As a result, it holds that $t_{ads} \propto 1/s_0$.

For molecular diffusion in a trench, the ratio between the diffusion time and adsorption time can be calculated by $\frac{t_{diff}}{t_{ads}} = \frac{3}{4} s_0 \left(\frac{L}{h}\right)^2$ or more roughly as $\frac{t_{diff}}{t_{ads}} \approx s_0 \text{AR}^2$.[1] Although the formal derivation is not so straightforward, this expression can be understood using the proportionalities $t_{diff} \propto \text{AR}^2$ and $t_{ads} \propto 1/s_0$ explained above. For low values of $s_0 \text{AR}^2$, roughly when $s_0 \text{AR}^2 < 0.01$, diffusion is much faster than adsorption and we have reaction-limited growth. On the other side, when $s_0 \text{AR}^2 > 100$, film growth is diffusion-limited.

We will now discuss these two cases using the animations below, showing cross-sectional side views of ALD in a trench. Here, the trench is oriented horizontally for clarity and for comparison with the PillarHall™ lateral-high-aspect-ratio trench structures used in our experiments (PillarHall™ LHAR generation 3 and 4, developed by Puurunen and co-workers and supplied by VTT Technical Research Centre of Finland).[1,2,9–11] Such a PillarHall™ structure is illustrated in figure 4. In the following animations, the gas-phase reactant density, scaled from 0 to 1, is plotted in a blue line. The surface coverage θ, which in the end determines the thickness of the deposited film, is indicated as a red outline on the surface of the trench.

Top view (experiment):

PillarHall™ LHAR4

768 μm

15 mm

distance / thickness

Cross-sectional side view (model):

Gas-phase reactant density   Surface coverage θ
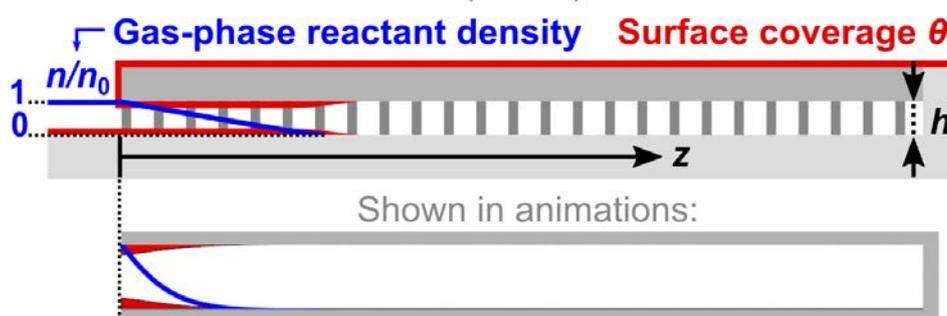
n/n_0

Shown in animations:

Figure 4: Pictures of PillarHall™ horizontal trench structures (top) supplied by VTT that we used in our experiments, where the silicon membrane is removed and the deposited film is visible. The schematic cross section of the structure (middle) shows the gas-phase reactant density (blue line) and surface coverage (red outline) in the same way as in the animations provided in this blog post (bottom).

The first animation, where $s_0\text{AR}^2 = 0.01$, corresponds to reaction-limited growth. For a complete representation of the growth process, this animation is split up into a 'short timescale' part and a 'long timescale' part. In real life, these stages roughly take microseconds and seconds, respectively, depending on the experimental conditions. In the short timescale part, we can see the blue line moving into the trench, up to the point where it has the same value everywhere. This corresponds to the diffusion of gas-phase reactant molecules into the trench until they are distributed uniformly. In the long timescale part, we can see that this results in a uniform increase in surface coverage, as indicated by the red outline.

$s_0\text{AR}^2=0.01$ **Short timescale (~μs)** Long timescale (~s)
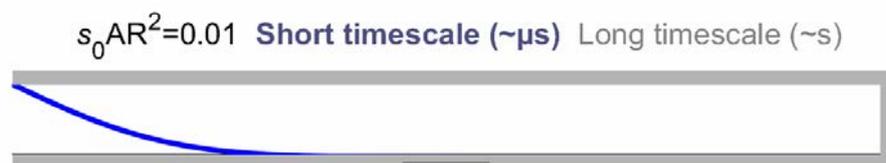
Animation 1 [Not playing in PDF]: Simulation of reaction-limited growth, with $s_0\text{AR}^2 = 0.01$. In all animations in this blog post, the red outline represents the surface coverage and the blue line corresponds to the gas-phase reactant density inside the trench. Furthermore, a small time line is included at the bottom to indicate the progression of the animation.

Because of the uniform growth rate during reaction-limited growth, the reactant dose needed to reach film saturation in the high-AR structure is the same as that for a planar substrate. Correspondingly, the saturation dose is proportional to $\frac{1}{A_0 s_0}$, where A_0 is average effective area per adsorption site.[2,5,6] In figures 1 and 3, this area A_0 corresponds to the area of one square, representing one adsorption site.

The next animation corresponds to diffusion-limited growth. Here, $s_0\text{AR}^2 = 1000$ such that the reactant molecules already adsorb before they can diffuse deep into the trench. As a result, film saturation is reached close to the entrance, while the surface is still 'empty' deeper inside the trench. Subsequently, in the saturated region near the entrance, the reactant molecules are no longer lost through adsorption and can therefore diffuse toward the 'adsorption front' where empty adsorption sites are still available. Accordingly, film growth is propagating increasingly deep into the trench.


Animation 2 [Not playing in PDF]: Simulation of diffusion-limited growth, with $s_0\text{AR}^2 = 1000$.

Note that the penetration depth of the deposited film is not determined by the time during which the reactant molecules can diffuse, but rather by the number of reactant molecules that are supplied into the trench. This is because the adsorption sites have to be 'filled up' in order to reach this depth, as indicated in figure 3 (right), for which also a certain number of reactant molecules is needed. The penetration depth therefore scales with the reactant dose, so reactant pressure times dosing time. This is not a linear relation, since not every molecule that diffuses randomly inside the trench also makes it to an adsorption site: it can also move out of the trench. As a result of this random walk diffusion, the penetration depth of the deposited film scales as $\text{PD}^{50\%} \propto h\sqrt{A_0\text{Dose}}$,[5,11] where $\text{PD}^{50\%}$ is the so-called half-thickness-penetration-depth.[4,11] Note that when A_0 is larger, there are less adsorption sites on the surface that need to be filled and the deposited film also penetrates deeper.

This expression for the film penetration depth during diffusion-limited growth can also be used to predict the saturation dose Dose_{sat}, as saturation is approximately reached when the penetration depth $\text{PD}^{50\%}$ is the same as the total length L of the trench. Therefore, $h\sqrt{A_0\text{Dose}_{sat}} \propto L$, which using $\text{AR} = L/h$ gives that $\text{Dose}_{sat} \propto \frac{1}{A_0}\text{AR}^2$.[5,6] Note that here the saturation dose is not affected by the reactivity of the reactant, but only by the aspect ratio and the number of adsorption sites. This explains the success of the Gordon model in predicting the saturation dose for diffusion-limited growth, while assuming a sticking probability of 1.[5]

Although the value of the initial sticking probability does not affect the penetration depth during diffusion-limited growth, it does affect the shape of the coverage profile. This is illustrated in the animation given below, where the surface coverage is plotted as a function of scaled distance z/h into the trench. If the gas-phase reactant molecules are very 'sticky', they are most likely to adsorb directly at the adsorption front where they first encounter empty adsorption sites. In contrast, if the value of s_0 is lower, the reactant molecules can scatter around more often before they adsorb, such that the adsorption front is more spread out. Note that this 'sharpness' of the front remains the same as a function of reactant dose and is, in first approximation, only determined by the value of s_0. This relation can therefore be used to experimentally determine the value s_0 corresponding to the half-cycle with the lowest penetration depth, as explained in our paper "*Sticking probabilities of H₂O and Al(CH₃)₃ during atomic layer deposition of Al₂O₃ extracted from their impact on film conformality*".[1]
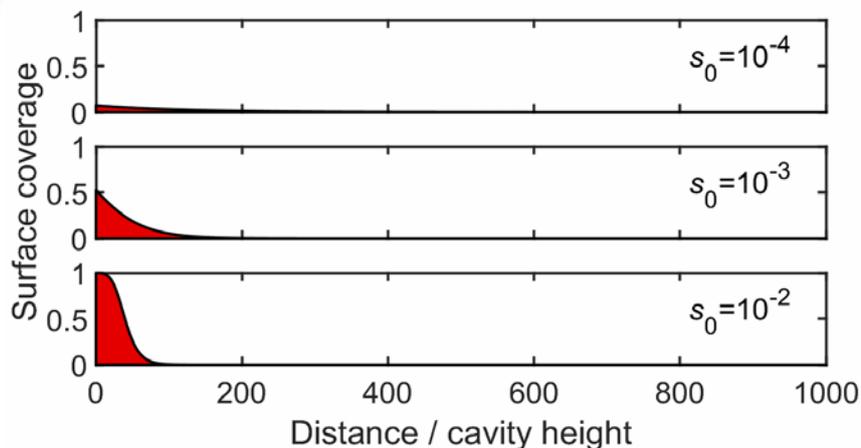
Animation 3 [Not playing in PDF]: Surface coverage versus distance into a trench during diffusion-limited growth, for different values of the initial sticking probability.

Plasma ALD: recombination-limited growth

For plasma ALD the conformality story becomes a bit more difficult. As explained in the 'modeling ALD conformality' section, plasma radicals that are diffusing into a trench can also be lost through recombination, as expressed by the surface recombination probability r, rather than by adsorption only. The presence of recombination loss typically results in recombination-limited growth, where the penetration depth of the reactant species (here, plasma radicals) into the high-AR structure is limited by recombination.

To determine whether film growth is recombination-limited, the value of $r\text{AR}^2$ can be used. Similar to the parameter $s_0\text{AR}^2$, discussed in the previous section, the value of $r\text{AR}^2$ represents the ratio between the diffusion time and recombination time. When $r\text{AR}^2 \gg 1$, the plasma radicals recombine before they can diffuse to the end of the trench, such that film growth is recombination-limited. When $r\text{AR}^2 < 1$, the plasma radicals can reach the end of the trench and provide reaction-limited or diffusion-limited growth, depending on the value of $s_0\text{AR}^2$. Note that in this case the penetration depth of the deposited film may be limited by the precursor half-cycle rather than the plasma half-cycle.

In the following animations, we can see how the value of $r\text{AR}^2$ affects the film growth. Here, $s_0\text{AR}^2$ is kept constant at 1000 and $r\text{AR}^2$ is varied from 100 to 1000 and 10000, such that film growth is recombination-limited in all three cases. Most strikingly, it can be seen that the penetration depth of the plasma radicals, and therefore that of the deposited film, is higher for lower values of the recombination probability. For $r\text{AR}^2 = 100$, film growth eventually reaches about halfway of the trench, while for $r\text{AR}^2 = 10000$ only the first ~5% of the structure is coated. As a rule of thumb, a high-AR structure can still be coated rather easily when $r\text{AR}^2 \approx 1$. Or in other words, the aspect ratio that is easily reached during a plasma ALD process can be estimated by $\text{AR}_{easy} \approx 1/\sqrt{r}$. In our work, we have determined that $r \approx 6 \cdot 10^{-5}$ for plasma ALD of SiO₂ and TiO₂, such that film growth up to AR $\approx$ 900 was achieved using extended plasma steps.[2] This demonstrates that also plasma ALD can yield very conformal films.

Animation 4 [Not playing in PDF]: Simulation of recombination-limited growth for different values of $r\mathrm{AR}^2$ and a fixed value of $s_0\mathrm{AR}^2 = 1000$.

Let's have a closer look at overall growth behavior during recombination-limited growth. Again, the animations shown above are split up in two parts. In the 'short timescale' part, the radicals diffuse into the trench and are simultaneously being lost to the sidewalls through adsorption reactions and recombination reactions. In the 'long timescale' part, we can observe how recombination loss affects the film growth. First, saturation in surface coverage is reached in the region near the entrance of the trench. As adsorption loss no longer takes place in this saturated region, the radicals can move more deeply into the trench. Still, recombination loss continues, also on the saturated surface, and therefore eventually limits the depth up to which the radicals can diffuse. At that point a balance is formed between the flux of radicals moving into the trench and the persisting loss of radicals through surface recombination. This balance results in a steady state exponential decay in radical density, as indicated by the blue line.

Note that recombination loss is immediately dominant when $s_0\mathrm{AR}^2 \ll r\mathrm{AR}^2$, so also before saturation in surface coverage is reached in the beginning of the trench. Still, sooner or later the same exponential decay in radical density is also obtained when $s_0\mathrm{AR}^2 > r\mathrm{AR}^2$, as illustrated in the animations shown below. Therefore, the value of $s_0\mathrm{AR}^2$ affects the shape of the coverage profile, but has relatively limited effect on the penetration depth of the deposited film during recombination-limited growth.

Animation 5 [Not playing in PDF]: Simulation of recombination-limited growth for a fixed value of $r\mathrm{AR}^2$ and very different values of $s_0\mathrm{AR}^2$.

The exponential decay in radical density has a few practical consequences. As already mentioned, it limits the aspect ratio that can be coated relatively easily ($AR_{easy} \approx 1/\sqrt{r}$). Higher aspect ratios can also be reached, but it takes it takes exponentially more time to achieve film saturation deeper inside the high-AR structure. As a result, the dosing time needed to reach saturation on the entire structure increases exponentially with the aspect ratio. Moreover, the penetration depth of the deposited film increases logarithmically with the radical dose. This relation can be used to experimentally determine the value of r, as explained in our paper "*Film conformality and extracted recombination probabilities of O atoms during plasma-assisted atomic layer deposition of SiO₂, TiO₂, Al₂O₃ and HfO₂*".[2]

Concluding remarks

We hope that this blog post is helpful in explaining and understanding conformal film growth during (plasma) ALD. Please feel free to use the provided figures and animations in your presentations, with reference to this blog post (K. Arts, W.M.M. Kessels and H.C.M Knoops. Basic insights into ALD conformality – A closer look at ALD and thin film conformality. **2020**, 1. AtomicLimits).

Finally, I would like to end with a few take home messages:

- Sticking probabilities and surface recombination probabilities are important parameters determining film conformality during (plasma) ALD.
- In contrast to adsorption, surface recombination is persistent and therefore tends to be the dominant loss channel of reactive species during plasma ALD.
- For processes with a low surface recombination probability, also plasma ALD can provide exceptional film conformality.

References

(1) Arts, K.; Vandalon, V.; Puurunen, R. L.; Utriainen, M.; Gao, F.; Kessels, W. M. M. (Erwin); Knoops, H. C. M. Sticking Probabilities of H2O and Al(CH3)3 during Atomic Layer Deposition of Al2O3 Extracted from Their Impact on Film Conformality. *J. Vac. Sci. Technol. A* **2019**, *37* (3), 030908. https://doi.org/10.1116/1.5093620.

(2) Arts, K.; Utriainen, M.; Puurunen, R. L.; Kessels, W. M. M.; Knoops, H. C. M. Film Conformality and Extracted Recombination Probabilities of O Atoms during Plasma-Assisted Atomic Layer Deposition of SiO2, TiO2, Al2O3, and HfO2. *J. Phys. Chem. C* **2019**, *123* (44), 27030–27035. https://doi.org/10.1021/acs.jpcc.9b08176.

(3) Knoops, H. C. M.; Langereis, E.; van de Sanden, M. C. M.; Kessels, W. M. M. Conformality of Plasma-Assisted ALD: Physical Processes and Modeling. *J. Electrochem. Soc.* **2010**, *157* (12), G241–G249. https://doi.org/10.1149/1.3491381.

(4) Cremers, V.; Puurunen, R. L.; Dendooven, J. Conformality in Atomic Layer Deposition: Current Status Overview of Analysis and Modelling. *Appl. Phys. Rev.* **2019**, *6*, 021302. https://doi.org/10.1063/1.5060967.

(5) Gordon, R. G.; Hausmann, D.; Kim, E.; Shepard, J. A Kinetic Model for Step Coverage by Atomic Layer Deposition in Narrow Holes or Trenches. *Chem. Vap. Depos.* **2003**, *9* (2), 73–78.

(6) Yanguas-Gil, A.; Elam, J. W. Self-Limited Reaction-Diffusion in Nanostructured Substrates: Surface Coverage Dynamics and Analytic Approximations to ALD Saturation Times. *Chem. Vap. Depos.* **2012**, *18* (1–3), 46–52. https://doi.org/10.1002/cvde.201106938.

(7) Knoops, H. C. M.; Elam, J. W.; Libera, J. A.; Kessels, W. M. M. Surface Loss in Ozone-Based Atomic Layer Deposition Processes. *Chem. Mater.* **2011**, *23* (9), 2381–2387. https://doi.org/10.1021/cm2001144.

(8)   Elam, J. W.; Routkevitch, D.; Mardilovich, P. P.; George, S. M. Conformal Coating on Ultrahigh-Aspect-Ratio Nanopores of Anodic Alumina by Atomic Layer Deposition. *Chem. Mater.* **2003**, *15* (18), 3507–3517. https://doi.org/10.1021/cm0303080.

(9)   Gao, F.; Arpiainen, S.; Puurunen, R. L. Microscopic Silicon-Based Lateral High-Aspect-Ratio Structures for Thin Film Conformality Analysis. *J. Vac. Sci. Technol. A Vacuum, Surfaces, Film.* **2015**, *33* (1), 010601. https://doi.org/10.1116/1.4903941.

(10)   Puurunen, R. L.; Gao, F. Influence of ALD Temperature on Thin Film Conformality: Investigation with Microscopic Lateral High-Aspect-Ratio Structures. *2016 14th Int. Balt. Conf. At. Layer Depos. BALD 2016 - Proc.* **2016**. https://doi.org/10.1109/BALD.2016.7886526.

(11)   Ylilammi, M.; Ylivaara, O. M. E.; Puurunen, R. L. Modeling Growth Kinetics of Thin Films Made by Atomic Layer Deposition in Lateral High-Aspect-Ratio Structures. *J. Appl. Phys.* **2018**, *123*, 205301. https://doi.org/10.1063/1.5028178.